Gyrofluid models for turbulence and reconnection in space plasmas

T. Passot

with: S.S. Cerri, C. Granier, D. Laveder, P.L. Sulem, E. Tassi

UCA, CNRS, Observatoire de la Côte d'Azur, Nice, France

& G. Miloshevich

LSCE, CEA Gif-sur-Yvette, France

Colloque PNST

08-12 janvier 2024, Marseille, France

OUTLINE

0. A reduced gyrofluid model covering scales from the MHD to the sub-d_e ranges

I. RMHD cascades within the colliding wave-packets scenario

II. Focus on Alfvén wave direct cascade in the presence of imbalance for $\chi < 1$

III. Co- versus counter-propagating wave interactions
- theoretical considerations
- validation by simulations of plane wave collisions

IV. Limitations and perspectives

V. Conclusion

0. A reduced gyrofluid model covering scales from the MHD to the sub-d_e ranges

Hamiltonian two-field system retaining B_z fluctuations, ion FLRs, electron inertia was constructed from gyrofluid model of Brizard 1992 (PoFB 4, 1213). Scales must be large compared to ρ_e and thus β_e small enough.

Describes **3D quasi-perpendicular dynamics of AWs, KAWs and IKAWs** excluding slow (and fast) waves.
This model limits to known equations, from RMHD to EMHD.

The model reads *(T.P., Sulem & Tassi 2018, PoP 25, 042107)*

$$\begin{cases} \partial_t N_e + [\varphi, N_e] - [B_z, N_e] + \dfrac{2}{\beta_e}\nabla_\parallel \Delta_\perp A_\parallel = 0 \\ \partial_t\left(1 - \dfrac{2\delta^2}{\beta_e}\Delta_\perp\right)A_\parallel - \left[\varphi, \dfrac{2\delta^2}{\beta_e}\Delta_\perp A_\parallel\right] + \left[B_z, \dfrac{2\delta^2}{\beta_e}\Delta_\perp A_\parallel\right] + \nabla_\parallel(\varphi - N_e - B_z) = 0, \\ \left(\dfrac{2}{\beta_e} + (1+2\tau)(\Gamma_0 - \Gamma_1)\right)B_z = \left(1 - \left(\dfrac{\Gamma_0 - 1}{\tau}\right) - \Gamma_0 + \Gamma_1\right)\varphi \\ N_e = \left(\left(\dfrac{\Gamma_0 - 1}{\tau}\right) + \delta^2\Delta_\perp\right)\varphi - (1 - \Gamma_0 + \Gamma_1)B_z. \end{cases}$$

Quadratic invariants: Energy and generalized cross-helicity (GCH)

$$\boxed{\begin{aligned} \mathcal{E} &= \frac{1}{2}\int \left(\frac{2}{\beta_e}|\nabla_\perp A_\parallel|^2 + \frac{4\delta^2}{\beta_e^2}|\Delta_\perp A_\parallel|^2 - N_e(\varphi - N_e - B_z)\right)d^3x, \\ \mathcal{C} &= -\int N_e\left(1 - \frac{2\delta^2}{\beta_e}\Delta_\perp\right)A_\parallel d^3x. \end{aligned}}$$

with $\delta^2 = m_e/m_i$ $\quad \tau = T_{0i}/T_{0e}$ $\quad \nabla_\parallel f = -[A_\parallel, f] + \dfrac{\partial f}{\partial z}.$ $\quad [f,g] = \partial_x f \partial_y g - \partial_y f \partial_y g$

N_e: electron gyrocenter density fluctuations ($N_e = n_e - B_z$ at large scales) ; φ and $A_{//}$: electric and magnetic potentials.

The Γ_0 and Γ_1 operators stand for $\Gamma_n(-\tau\Delta_\perp)$ with $\Gamma_n(x) = I_n(x)e^{-x}$

I. RMHD cascades within the colliding wave-packets scenario

The simplicity of the model but also its richness allows a parametric study in complex situations

Reconnection mediated turbulence (RMT)

If current sheets sufficiently **thin** and **long-lived** (e.g. with dynamic alignment), they can be (recursively) **disrupted by reconnection**. When the tearing growth timescale becomes shorter than the eddy lifetime , a **tearing mediated range** is obtained, with a magnetic spectrum :$\simeq k_\perp^{-11/5}$ (see e.g. Boldyrev & Loureiro, ApJ 2017)

RMT was simulated in 2D (Dong et al. 2018). Dong et al., Sci. Adv. 8, eabn7627 (2022) observed it in 3D (10^4 x10^4 x 5x 10^3 grid cells and 200M CPUh).

Collisions of wave packets (Cerri et al. ApJ 939:36, 2022); 672^3 grid cells. Clear evidence of **3D RMT in MHD range** when **nonlinearities are weak**.

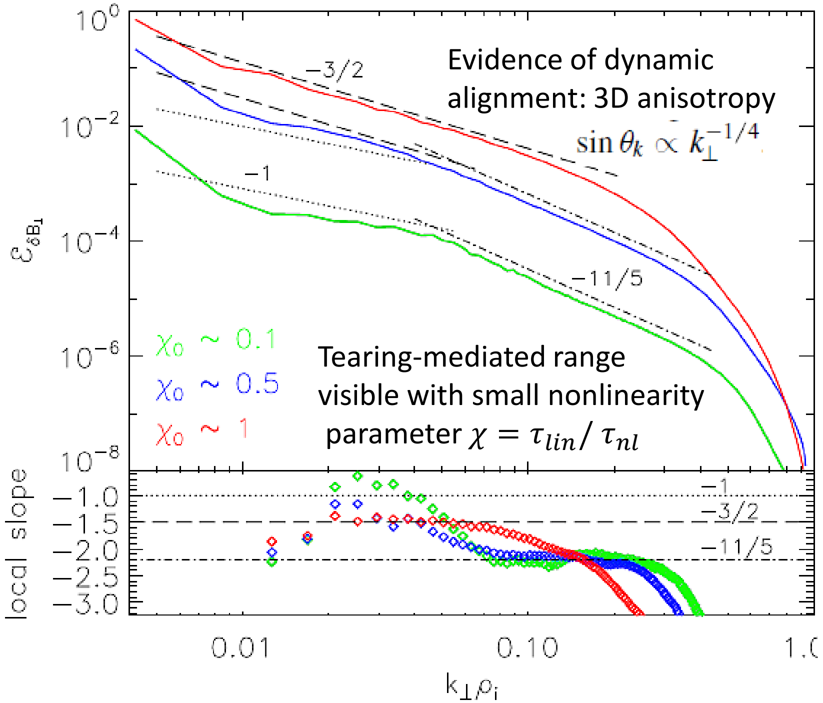

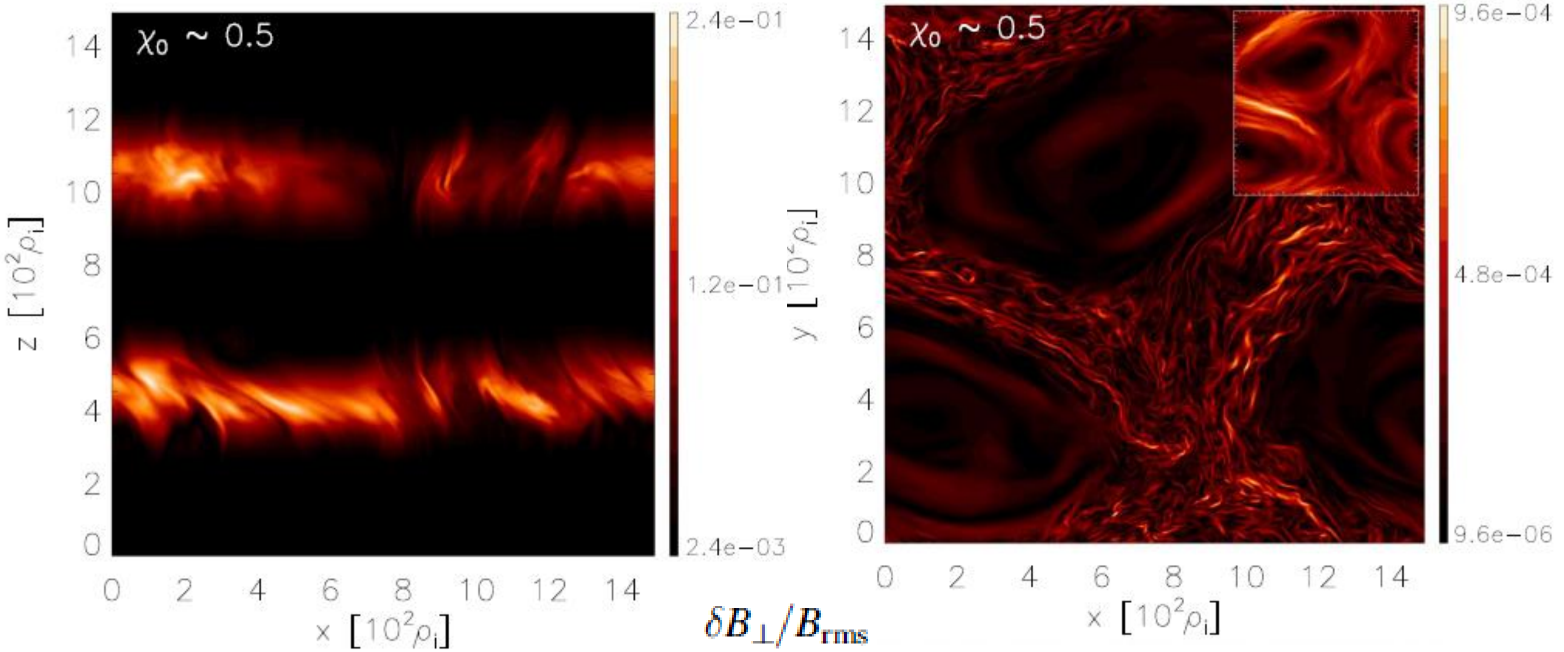

II. Alfvén wave cascades in the presence of imbalance

At scales **larger** than the ion gyroradius, GCH identifies with MHD cross-helicity and undergoes a **direct cascade**.
At **smaller** scales, GCH becomes magnetic helicity and undergoes an **inverse cascade** (*Miloshevich et al. JPP 87, 905870201, 2021).*

➔ Investigate how the energy and cross-helicity cascade across the transition between the MHD and the sub-ion ranges.

Summary of past work

Meyrand et al. (JPP 2021) : 2-field FLR-MHD with β_e <<1, driven by negative damping with non-zero CH.
Stationary regime with large imbalance and large χ (ratio of nonlinear to linear frequencies), *breaking the asymptotics of gyrofluid models.*

Reveals a **helicity barrier** at ion scale with :

– **depletion of energy flux** towards small perpendicular scales
– energy accumulates at large scales and **transfers in parallel direction at ion perpendicular scale**
resulting in
– **steepening** of energy (and magnetic) **spectra** in the **"transition range"**

– imbalance increases; saturation through parallel dissipation **(non-universality)**

In **kinetic simulation** of *Squire et al. Nature Astro. (2022) at* β_e = 0.3 dissipation is seen to originate from **ion-cyclotron resonance.**
Consistent with solar wind observations (Bowen et al. 2022 & 2023).

Critical balance and requirement that $k_\| d_i = 1$ (d_i = ion inertial length) at $k_\perp \rho_i = 1$ (ρ_i = ion Larmor radius), suggests saturation amplitude scaling like $\beta_i^{1/2}$.

This work focuses on the regime χ < 1 *(consistent with underlying gyrofluid scaling)* *TP & al. JPP **88**, 905880312 (2022)*

Simulation at moderate β_e, driven by freezing the amplitude of modes with transverse wavenumbers in the first spectral shell and k_z (L/2π) = ±1

Permits simulations with high imbalance and a moderate nonlinearity parameter;
Injection rates of energy and of GCH are not prescribed but are nevertheless constant on average in stationary phase.

Small-scale regularization by hyper-dissipation operator $\nu_\perp(\Delta_\perp)^4 + \nu_z\partial_z^8$ acting on N_e and $A_\parallel$, supplemented in the corresponding equations.

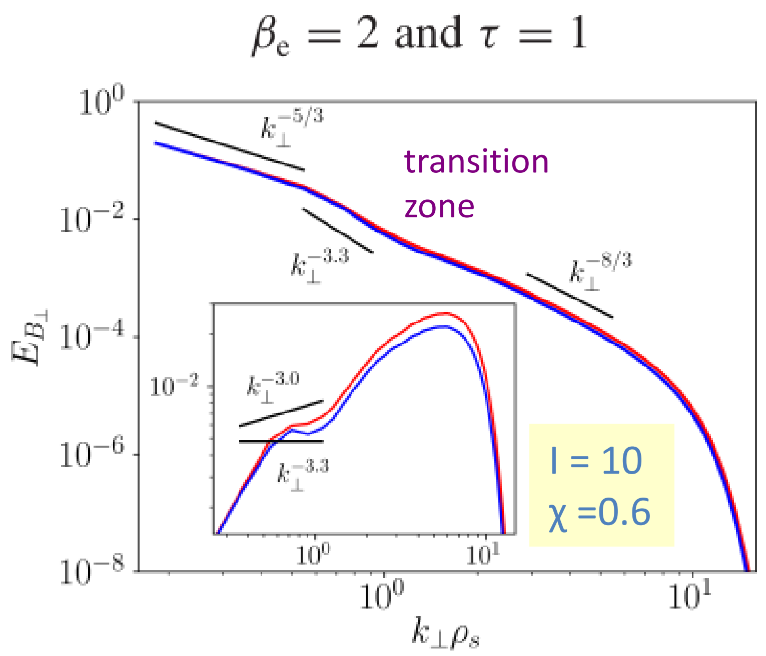

Transverse magnetic energy spectra for two time-intervals

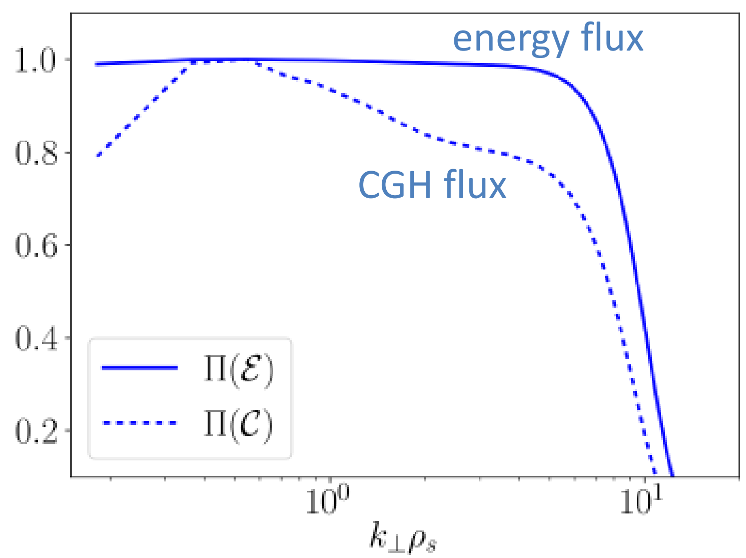

Energy flux keeps almost constant when crossing helicity barrier.

Influence of imbalance on $E^\pm(k_\perp)$

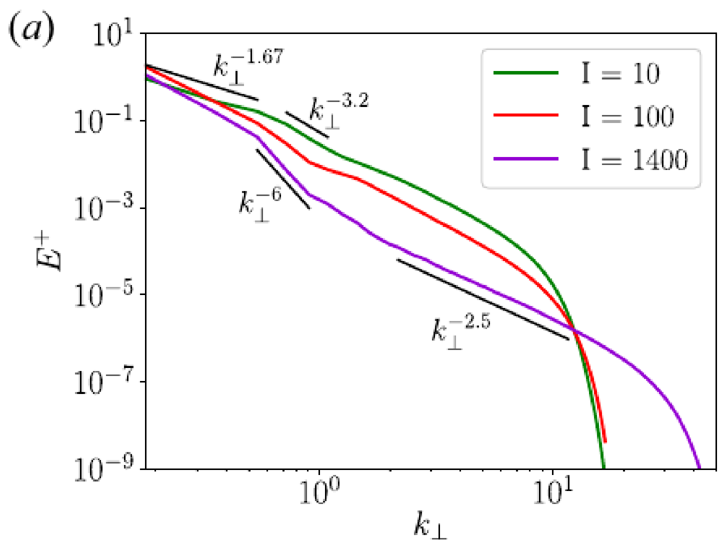

Larger imbalance steepens the transition range, consistent with solar wind observations reported in *Huang et al. ApJL **909**, L7 (2021)*

Presence of a transition zone near the ion scale;
persists when parallel viscosity is set to zero

III. Co- versus counter-propagating wave interactions

Investigate if, at small χ, the transition range can result from **co-propagating wave interactions**

(cf. Voitenko & De Keyser NPG 2011; ApJL 2016)

Analysis of the interaction times

Characteristic nonlinear interaction rate in the MHD, WD (weakly dispersive) and SD (strongly dispersive) ranges

- **counter-propagating waves:**

$$\gamma_k^{NL} \simeq \begin{cases} k_\perp B_k & (MHD\ range) \\ k_\perp B_k & (WD\ range) \\ k_\perp^2 B_k & (SD\ range) \end{cases}$$

- **co-propagating waves:**

$$\gamma_k^{NL} \simeq \begin{cases} 0 & (MHD\ range) \\ k_\perp^3 B_k & (WD\ range) \\ k_\perp^2 B_k & (SD\ range) \end{cases}$$

Can be estimated using KAW parametric decay growth rate γ_k given by:

$$\gamma^2(k_\perp) = \frac{1}{64}\frac{(\widehat{\boldsymbol{z}}\cdot(\boldsymbol{p}\times\boldsymbol{q}))^2}{\xi(p_\perp)\xi(q_\perp)}\frac{1}{k_\perp^2 p_\perp^2 q_\perp^2}\left(\frac{\sigma_k}{\xi(q_\perp)}-\frac{\sigma_q}{\xi(k_\perp)}\right)\left(\frac{\sigma_p}{\xi(k_\perp)}-\frac{\sigma_k}{\xi(p_\perp)}\right)$$
$$\times\left(\sigma_k k_\perp^2\xi(k_\perp)+\sigma_p p_\perp^2\xi(p_\perp)+\sigma_q q_\perp^2\xi(q_\perp)\right)^2|a_k^{\sigma_k}|^2, \qquad (15)$$

(Miloshevich et al. (2021) JPP 87, 905870201) where $|a_k^{\sigma_k}|^2 = (8/\beta_e)|B_\perp(\boldsymbol{k})|^2$

Resulting Kolmogorov spectra in WDR

Strong turbulence:
$E_B(k_\perp)\sim k_\perp^{-3}$ (Voitenko & De Keyser, NPG 2011),

Weak turbulence (relevant for large imbalance):
$E_B(k_\perp)\sim k_\perp^{-4}$

Validation using simulations of co- versus counter-propagating plane wave interactions

(Cerri et al., in preparation; TP et al. : arxiv.org/abs/2401.03863)

Kinetic-Alfvén plane waves with $\tau = 8$; $\beta = 0.0625$; $\delta = 0$ and $L / 2\pi\rho_s = 4$ $(\rightarrow L / 2\pi\rho_i = 1)$
Laplacian + hyper (ηk^8) dissipation

We focus on the two cases.
counter-propagating waves with:

$$\boldsymbol{k}^- = (\tfrac{1}{4}, 0, \tfrac{1}{4}),\ \boldsymbol{k}^+ = (0, \tfrac{1}{2}, -\tfrac{1}{2})$$

and co-propagating waves with:

$$\boldsymbol{k}^- = (\tfrac{1}{4}, 0, \tfrac{1}{4}),\ \boldsymbol{k}^+ = (0, \tfrac{3}{4}, \tfrac{1}{2})$$

Nonlinear parameters:
$\chi \approx 0.8$ (decays to 0.65)

Quasi-steady state phase

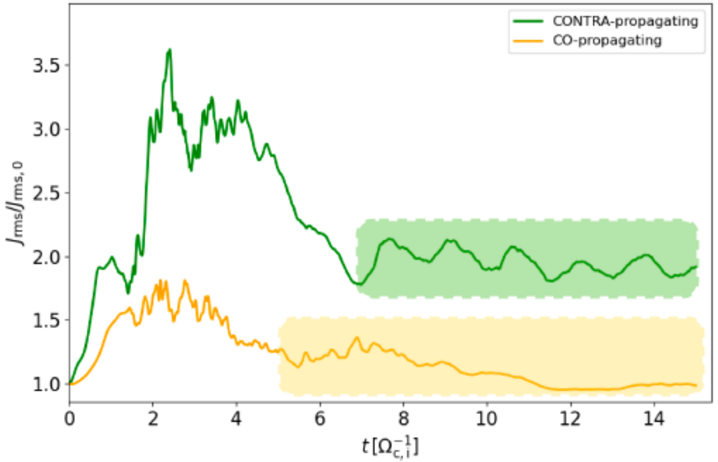

Co-propagating case displays steep transition range $\propto k_\perp^{-4}$

compensated by $k^{-8/3}$

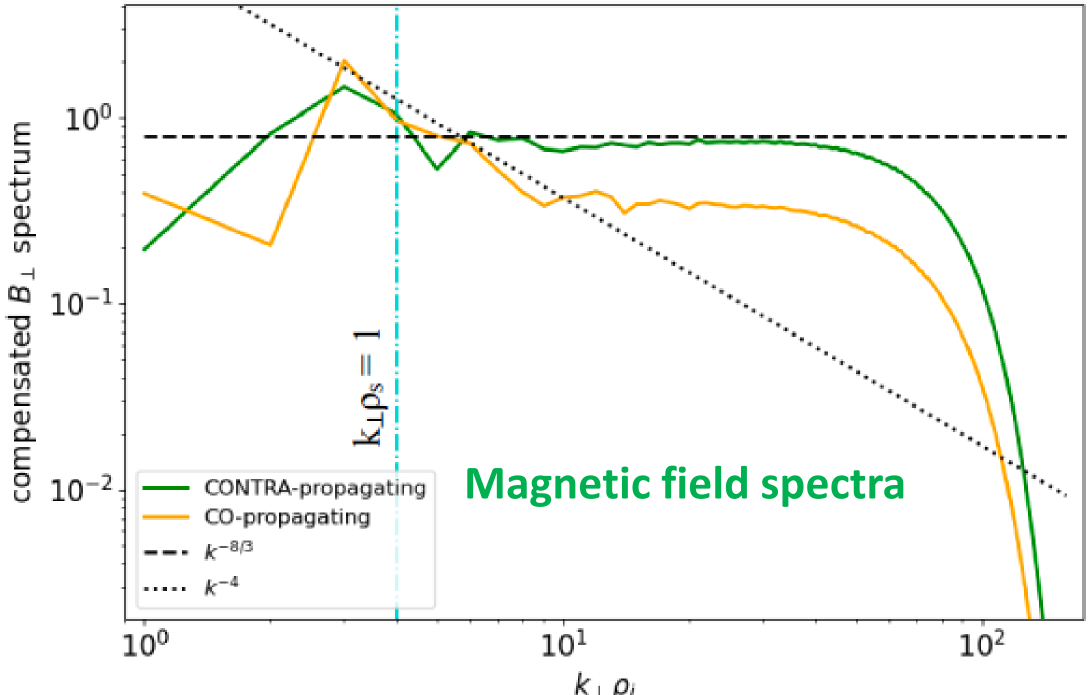

Time-averaged quantities

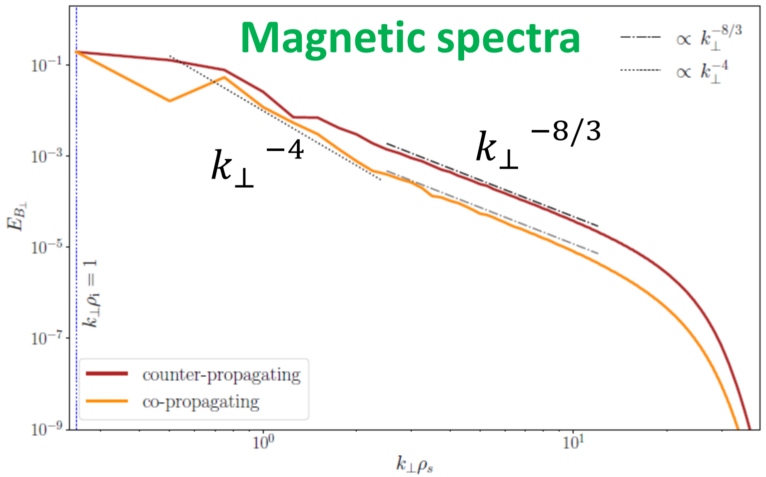

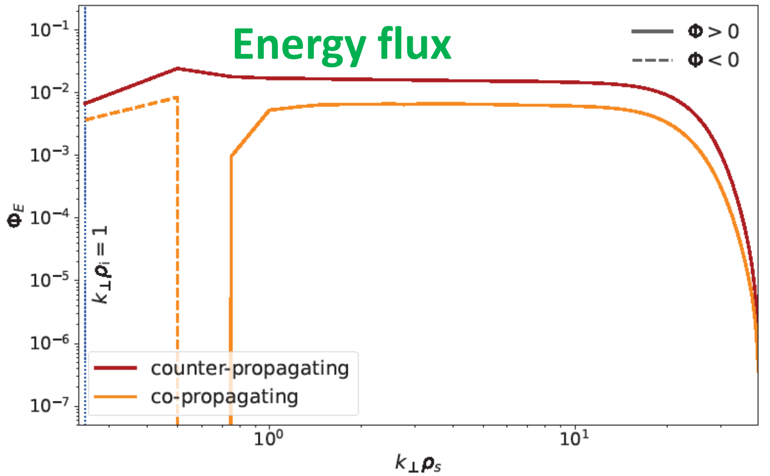

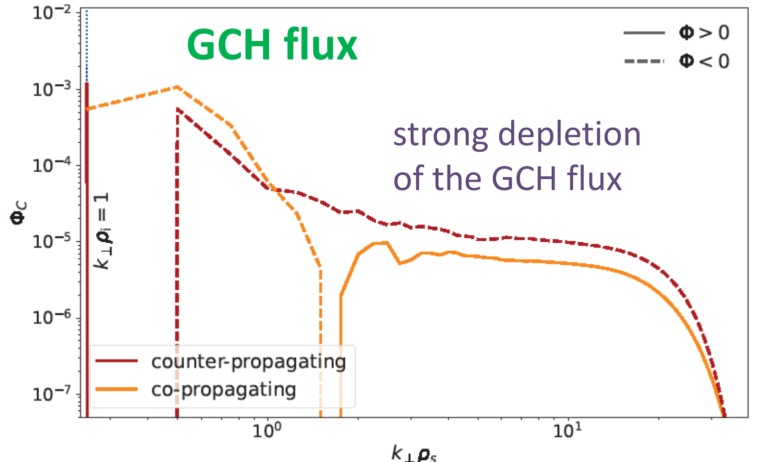

Co-propagating

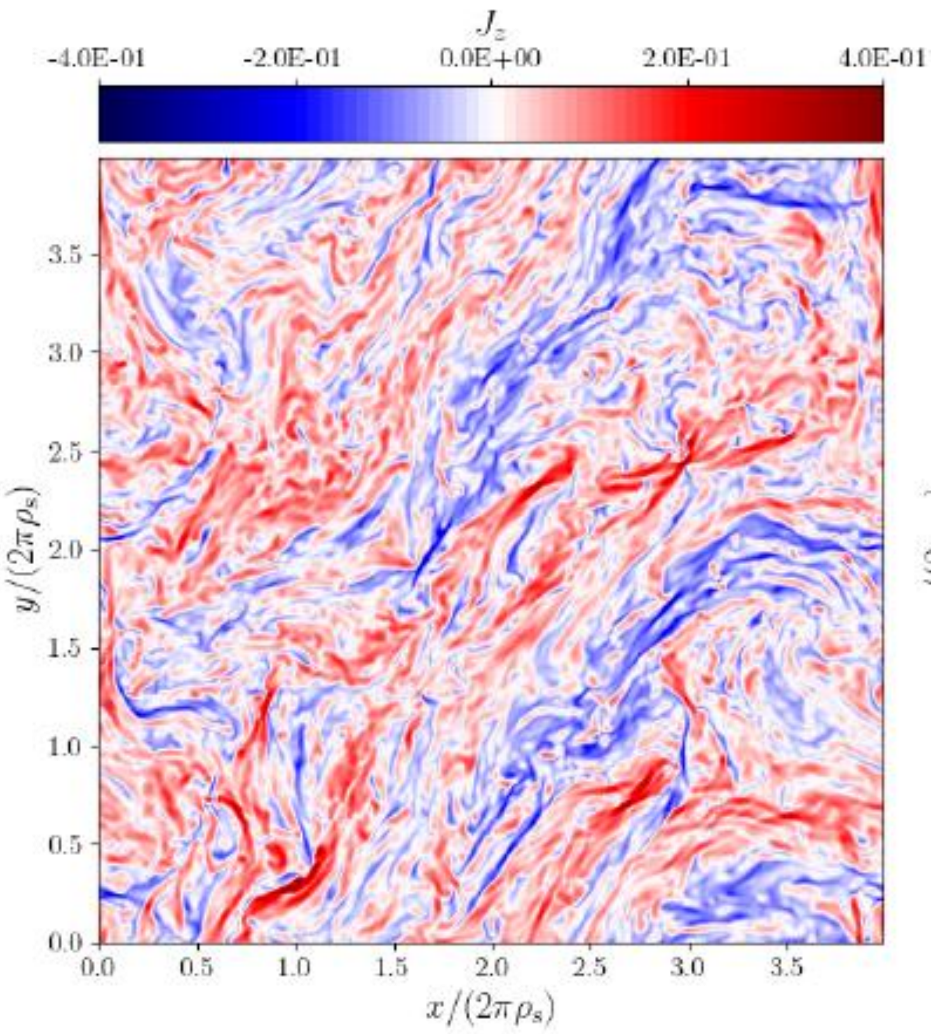

Counter-propagating

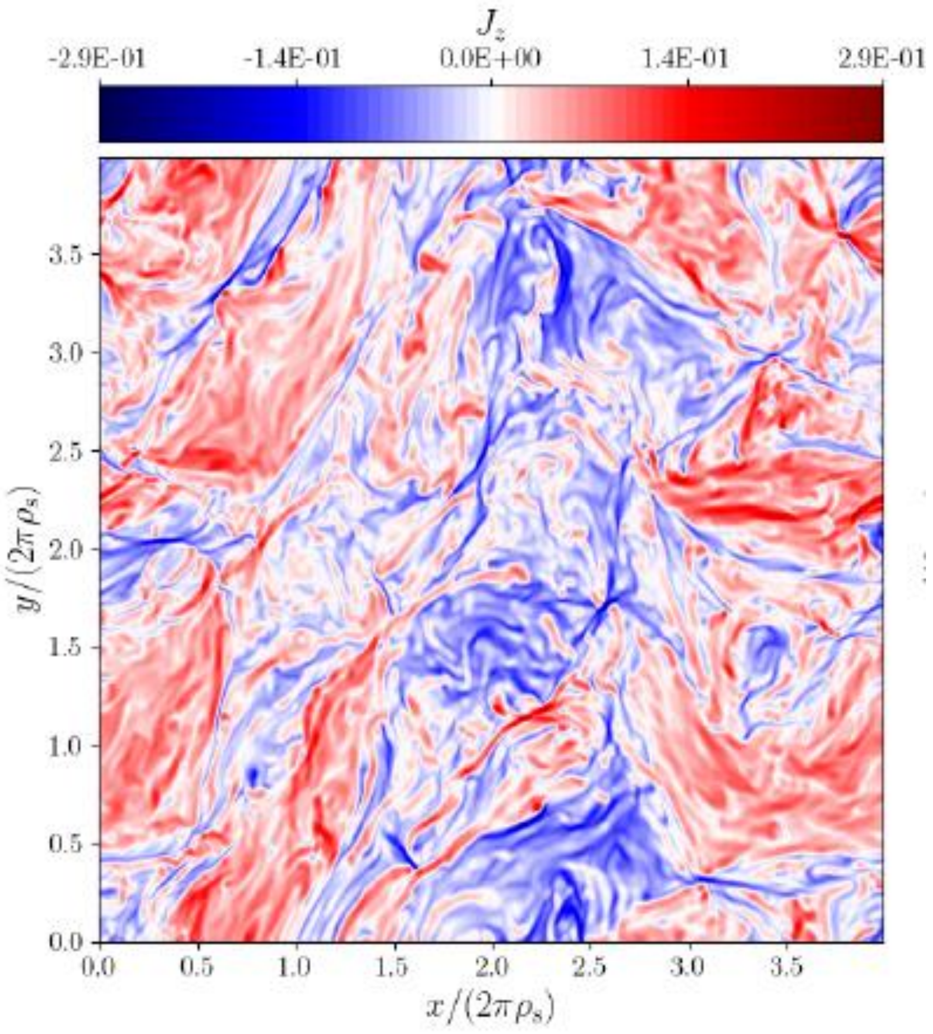

Smoother dynamics in the case of co-propagating waves

III. Limitations and perspectives

2D simulations of homogeneous turbulence in a domain of size $8\pi\rho_s$ displaying **collisionless reconnection and Kelvin-Helmholtz instability** with

$$\tau = 1; \;\; \beta_e = 0.02$$

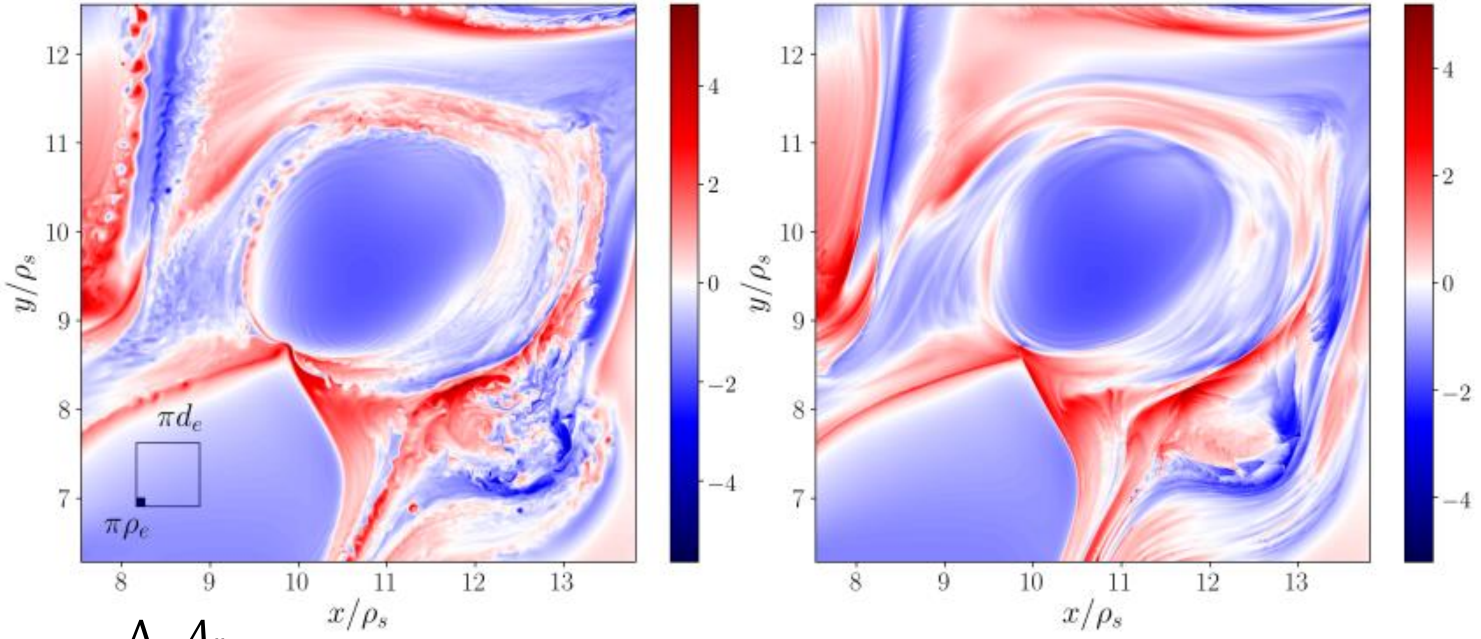

$\Delta_\perp A_\parallel$

With eFLR term

Without eFLR term

Electron FLR term smooths the dynamics and permits the development of KH instability

$$N_e = \left(\frac{\Gamma_0 - 1}{\tau} + \boxed{\delta^2 \Delta_\perp}\right)\varphi - (1 - \Gamma_0 + \Gamma_1) B_z.$$

At later times (with the eFLR term)

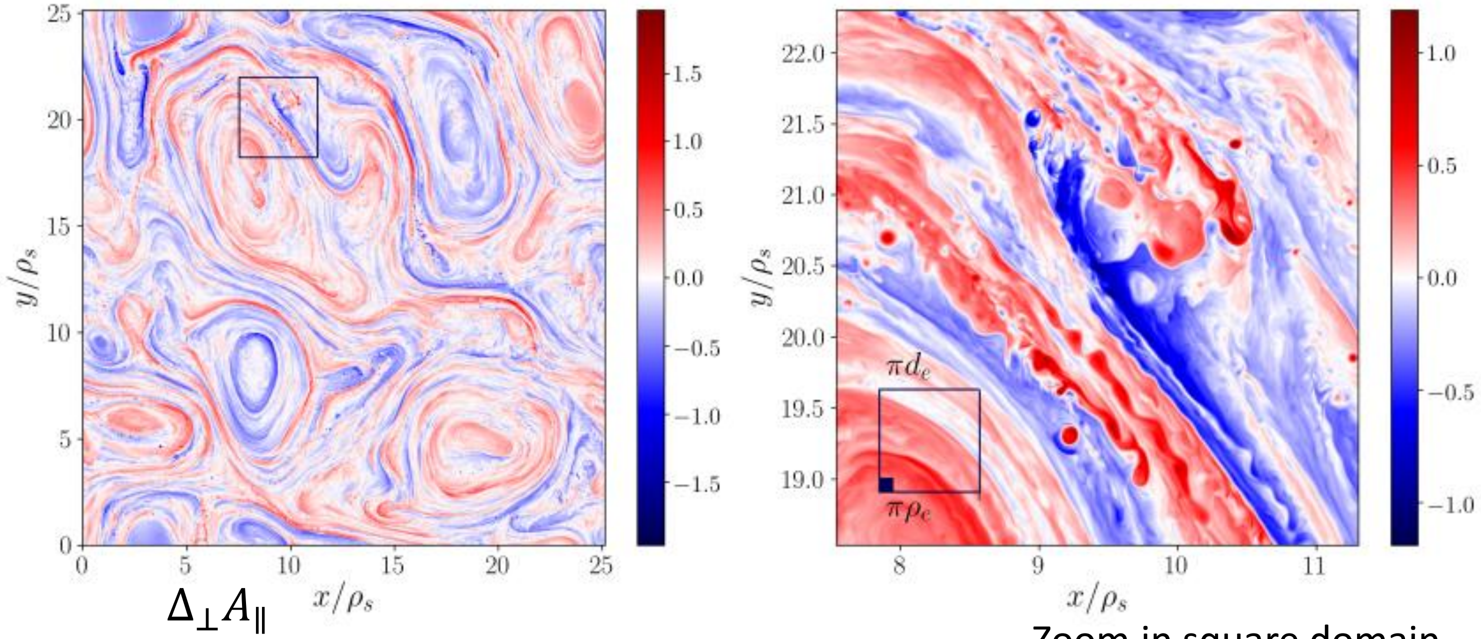

Zoom in square domain shown on left panel

Rich dynamics with steeper spectra at sub-electron scales (see e.g. Huang et al. ApJL 2014)

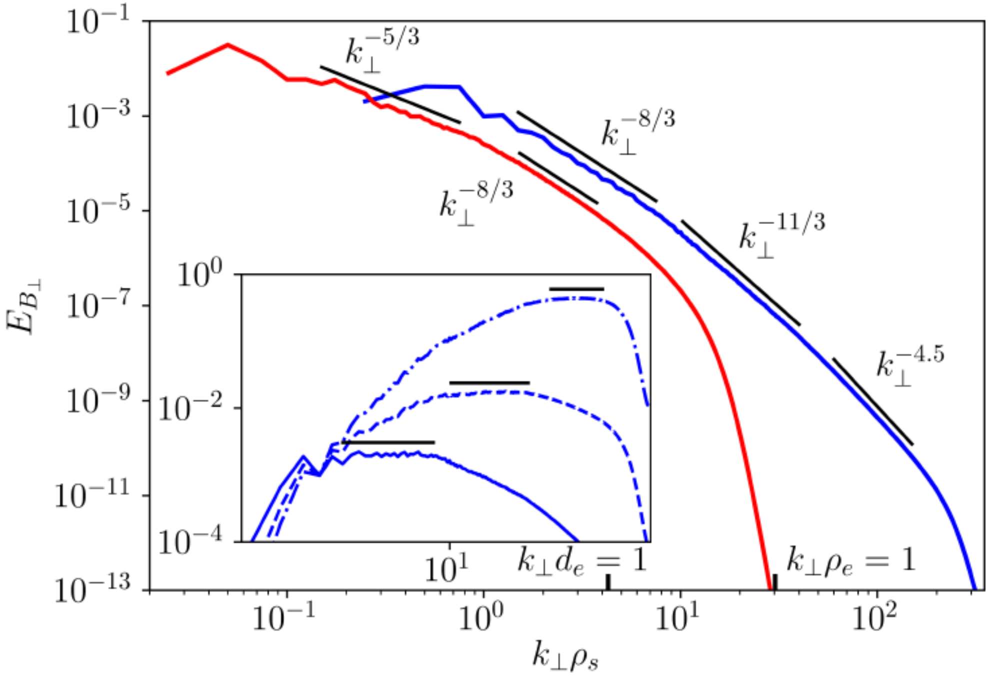

Since electron FLR terms are not fully described, there is a need for a more complete model.

V. Conclusion

The two-field model provides a paradigm to study KAW turbulence from MHD to electron scales, excluding other waves.

Perspectives:

- Study of reconnection mediated turbulence at sub-ion scales

A recently derived 4-field model (TP et al. submitted & Tassi et al. JPP 2020) includes **full ion and electron FLR** and restores the coupling to slow waves (important near ion scale are $\beta_e \approx 1$).

- Simulations of this model are planned.

Supplementary slides

Four-field model

$$\frac{\partial N_e}{\partial t} + [G_{10e}\varphi - \rho_s^2 2G_{20e}B_z, N_e] - [G_{10e}A_\|, U_e] + \frac{\partial U_e}{\partial z} = 0, \tag{A.1}$$

$$\frac{\partial}{\partial t}(G_{10e}A_\| - d_e^2 U_e) + [G_{10e}\varphi - \rho_s^2 2G_{20e}B_z, G_{10e}A_\| - d_e^2 U_e] + \rho_s^2[G_{10e}A_\|, N_e]$$
$$+ \frac{\partial}{\partial z}(G_{10e}\varphi - \rho_s^2(2G_{20e}B_z + N_e)) = 0, \tag{A.2}$$

$$\frac{\partial N_i}{\partial t} + [G_{10i}\varphi + \tau\rho_s^2 2G_{20i}B_z, N_i] - [G_{10i}A_\|, U_i] + \frac{\partial U_i}{\partial z} = 0, \tag{A.3}$$

$$\frac{\partial}{\partial t}(G_{10i}A_\| + d_i^2 U_i) + [G_{10i}\varphi + \tau\rho_s^2 2G_{20i}B_z, G_{10i}A_\| + d_i^2 U_i] - \tau\rho_s^2[G_{10i}A_\|, N_i]$$
$$+ \frac{\partial}{\partial z}(G_{10i}\varphi + \rho_s^2(\tau 2G_{20i}B_z + N_i)) = 0, \tag{A.4}$$

$$G_{10i}N_i - G_{10e}N_e = \frac{1-\Gamma_0}{\tau}\frac{\varphi}{\rho_s^2} - (\Gamma_0 - \Gamma_1)B_z - (G_{10e}^2 - 1)\frac{\varphi}{\rho_s^2} + G_{10e}2G_{20e}B_z, \tag{A.5}$$

$$\Delta_\perp A_\| = G_{10e}U_e - G_{10i}U_i, \tag{A.6}$$

$$B_z = -\frac{\beta_e}{2}\left(\tau 2G_{20i}N_i + (\Gamma_0 - \Gamma_1)\frac{\varphi}{\rho_s^2} + 2\tau(\Gamma_0 - \Gamma_1)B_z\right.$$
$$\left. + 2G_{20e}N_e - G_{10e}2G_{20e}\frac{\varphi}{\rho_s^2} + 4G_{20e}^2 B_z\right). \tag{A.7}$$

Continuity and parallel momentum equations for electron and ion gyrocenters (N_e , U_e, N_i , U_i)

FLR terms: G_{10e} , G_{10i} G_{20e} , G_{20i}

G_{10e}= 2 G_{20e} multiply field in Fourier space by $\exp(-\left(\frac{\beta_e}{4}\right) d_e^2 k_\perp^2)$

G_{10i}= 2 G_{20i} multiply field in Fourier space by $\exp(-\tau\varrho_s^2 k_\perp^2/2)$

Quasineutrality (A.5)

Parallel Ampere's law (A.6)

Perpendicular Ampere's law (A.7)

Does not assume β_e small; compatible with an **adiabatic** closure for the **ion** gyrocenter fluid and an **isothermal electron** fluid

Invariants

KAW phase velocity
$$v_{ph}^2 \equiv \left(\frac{\omega}{k_z}\right)^2 = \frac{2}{\beta_e}\frac{k_\perp^2}{1+\frac{2\delta^2 k_\perp^2}{\beta_e}}\frac{1-\widehat{M}_1+\widehat{M}_2}{\widehat{M}_2}.$$

M_1 and M_2 are defined as $B_z = M_1\varphi, \quad N_e = -M_2\varphi,$

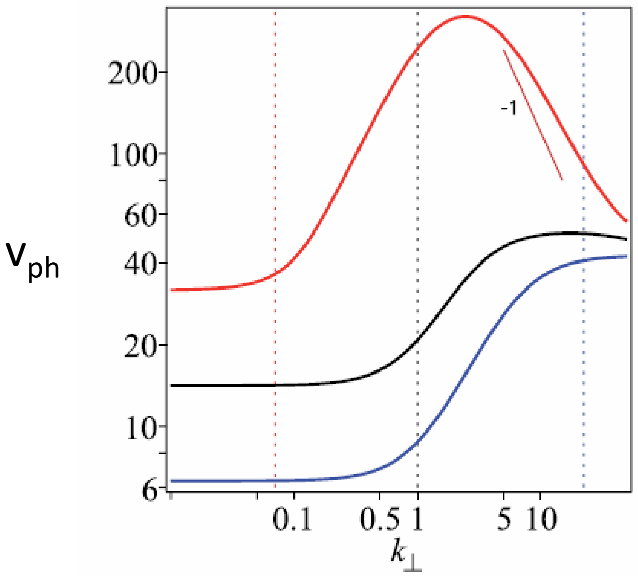

FIG. 1. Phase velocity of KAWs v_{ph} versus $k_\perp$ for $\beta_e = 0.002$, $\tau = 100$ (red), $\beta_e = 0.01$, $\tau = 0.5$ (black), and $\beta_e = 0.05$, $\tau = 0.001$ (blue). The vertical dotted lines refer to the inverse ion Larmor radius ρ_i^{-1} for the three values of τ,

Quadratic invariants:

$$\boxed{\begin{aligned}\mathcal{E} &= \frac{1}{2}\int\left(\frac{2}{\beta_e}|\nabla_\perp A_\|\|^2 + \frac{4\delta^2}{\beta_e^2}|\Delta_\perp A_\||^2 - N_e(\varphi - N_e - B_z)\right)d^3x,\\ \mathcal{C} &= -\int N_e\left(1-\frac{2\delta^2}{\beta_e}\Delta_\perp\right)A_\| d^3x.\end{aligned}}$$

Introducing the **generalized Elsasser potentials** (eigenmodes of the linearized system),

$$\boxed{\mu^\pm = \Lambda\varphi \pm sA_\|,}$$

where
$$\Lambda = D_e^{-1}(1+M_2-M_1)^{1/2}M_2^{1/2}$$
$$D_e^2 = (-\Delta_\perp)L_e$$
$$L_e = 1-\frac{2\delta^2}{\beta_e}\Delta_\perp,$$
$$s = (2/\beta_e)^{1/2}$$

the invariants read
$$\boxed{\begin{aligned}\mathcal{E} &= \frac{1}{4}\int\{(D_e\mu^+)^2 + (D_e\mu^-)^2\}\,dx.\\ \mathcal{C} &= \frac{1}{4}\int\left\{\left(V_{ph}^{-1/2}D_e\mu^+\right)^2 - \left(V_{ph}^{-1/2}D_e\mu^-\right)^2\right\}dx\end{aligned}}$$

Provides an interesting **generalization of cross-helicity at small scales.**

At large scales it reads $\mathcal{C} = -\int \boldsymbol{U}_{\perp i}\cdot\boldsymbol{B}_\perp d^3x$ while at sub-ions scales it identifies with **magnetic helicity**

The various limits: a unique model that limits to known equations from RMHD to EMHD

- **Hall-RMHD**

2-field reduction of 4-field model *of Schekochihin et al. (2009)* when neglecting u_i and assuming B_z slaved to φ.

$$\partial_t A_\| + \nabla_\| \left(\varphi - \frac{2}{\beta_e} \frac{1}{1+\frac{2}{\beta_e}} \Delta_\perp \varphi \right) = 0$$

$$\partial_t \Delta_\perp \varphi + [\varphi, \Delta_\perp \varphi] + \frac{2}{\beta_e} \nabla_\| \Delta_\perp A_\| = 0.$$

when $\tau k_\perp^2 \ll 1$, $\beta_e \lesssim 1$ and $\delta = 0$, $\tau \ll 1$

Without this dispersive term: **RMHD**

- **Model of *Schep, Pegoraro & Kuvshinov*** *(1994)*

$$\partial_t \left(1 - \frac{2\delta^2}{\beta_e}\Delta_\perp\right) A_\| - \left[\varphi, \frac{2\delta^2}{\beta_e}\Delta_\perp A_\|\right] + \nabla_\|(\varphi - \Delta_\perp \varphi) = 0$$

$$\partial_t \Delta_\perp \varphi + [\varphi, \Delta_\perp \varphi] + \frac{2}{\beta_e} \nabla_\| \Delta_\perp A_\| = 0.$$

when $\tau k_\perp^2 \ll 1$, $\beta_e \ll 1$ and $\delta \neq 0$, $\tau \ll 1$

- **REMHD** (dynamics of KAWs)

$$\partial_t A_\| + \nabla_\| \left(1 + \frac{1}{\tau}\right) \varphi = 0.$$

$$\partial_t \varphi - \frac{\frac{2\tau}{\beta_e}}{1 + \frac{\beta_e}{2}(1+\tau)} \nabla_\| \Delta_\perp A_\| = 0.$$

Schekochihin et al. 2009
Boldyrev et al. 2013

when $\tau k_\perp^2 \gg 1$, $\beta_e \lesssim 1$ and $\delta = 0$, $\tau \sim 1$

- Dynamics of **inertial KAWs** (*Chen & Boldyrev 2017; Passot et al. 2017*)

$$\partial_t \left(1 - \frac{2\delta^2}{\beta_e}\Delta_\perp\right) A_\| - \left[\varphi, \frac{2\delta^2}{\beta_e}\Delta_\perp A_\|\right] + \nabla_\| \varphi = 0$$

$$\partial_t \left(1 + \frac{2}{\beta_i} - \frac{2\delta^2}{\beta_e}\Delta_\perp\right) \varphi - \left[\varphi, \frac{2\delta^2}{\beta_e}\Delta_\perp \varphi\right] - \frac{4}{\beta_e^2} \nabla_\| \Delta_\perp A_\| = 0,$$

when $\tau k_\perp^2 \gg 1$, $\beta_e \ll 1$ and $\delta \neq 0$, $\tau \gg 1$

EMHD for whistlers is obtained when $\beta_i >> 1$

Driving at sub-ion scales

Neglecting electron inertia:

$$\partial_t N_e + [\varphi, N_e] - [B_z, N_e] + \frac{2}{\beta_e}\nabla_\parallel \Delta_\perp A_\parallel = 0,$$

$$\partial_t A_\parallel + \nabla_\parallel(\varphi - N_e - B_z) = 0.$$

$$\left(\frac{2}{\beta_e} + (1+2\tau)(\Gamma_0 - \Gamma_1)\right) B_z = \left(1 - \left(\frac{\Gamma_0 - 1}{\tau}\right) - \Gamma_0 + \Gamma_1\right)\varphi$$

$$N_e = \left(\frac{\Gamma_0 - 1}{\tau}\right)\varphi - (1 - \Gamma_0 + \Gamma_1)B_z.$$

Unbalanced driving at sub-ion scale scales

Energy is transferred to large scales (both perpendicular and parallel)

So are the positive and negative components of GCH.

GCH flux is constant and negative at scales larger than the injection scale.

INVERSE CASCADE OF GCH
(but not of energy)

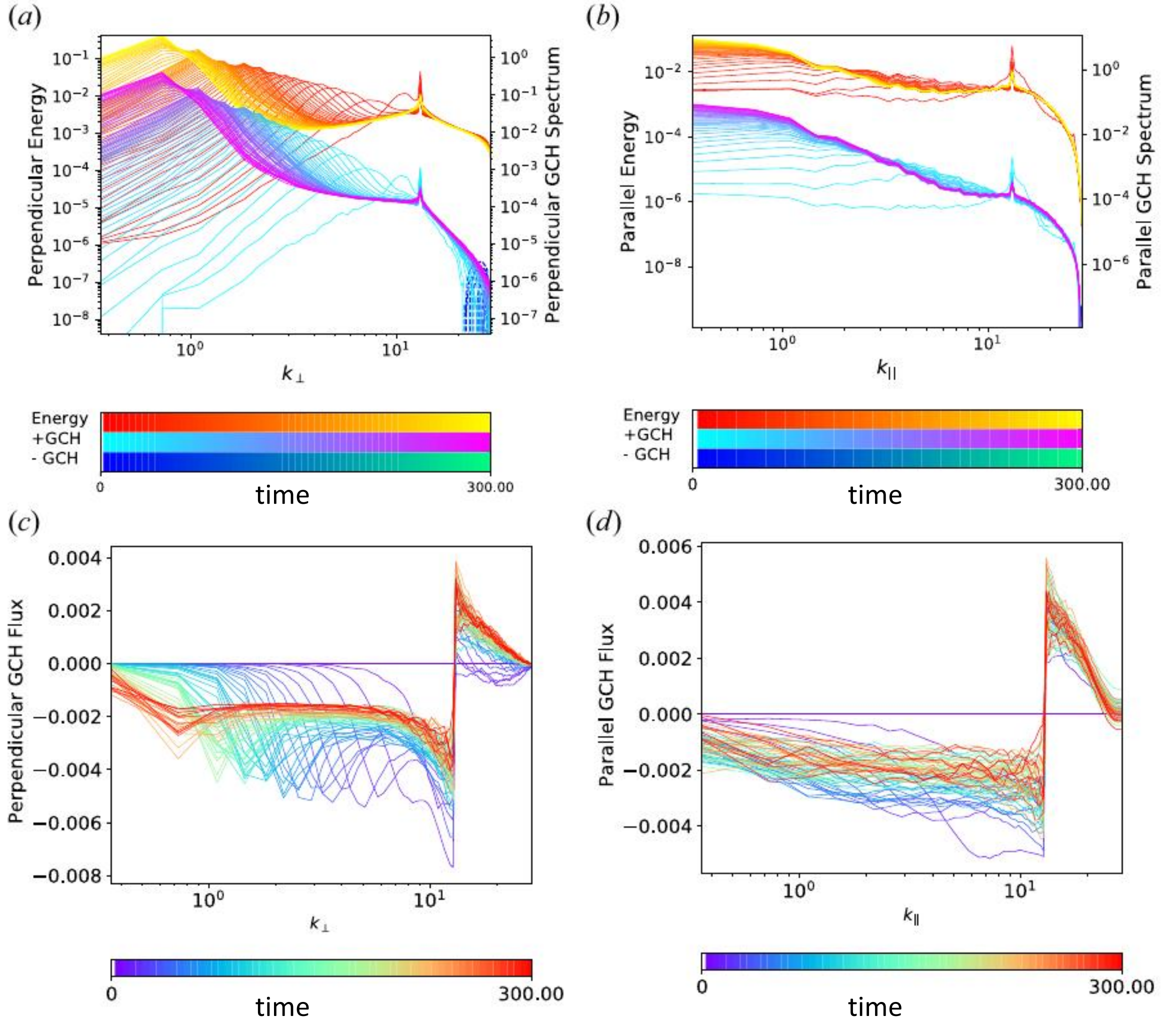

spectra

fluxes

Miloshevich, Laveder, Passot & Sulem
JPP ***87,*** *905870201, 2021.*